From Nanoscale Cohesion To Macroscale Entanglement: Opportunities For Designing Granular Aggregate Behavior By Tailoring Grain Shape And Interactions

Heinrich M. Jaeger, Marc Z. Miskin, Scott R. Waitukaitis

James Franck Institute and Department of Physics, The University of Chicago, 929 East 57th Street, Chicago, Illinois 60637, USA

Abstract. The packing arrangement of individual particles inside a granular material and the resulting response to applied stresses depend critically on particle-particle interactions. One aspect that recently received attention are nanoscale surface features of particles, which play an important role in determining the strength of cohesive van der Waals and capillary interactions and also affect tribo-charging of grains. We describe experiments on freely falling granular streams that can detect the contributions from all three of these forces. We show that it is possible to measure the charge of individual grains and build up distributions that are detailed enough to provide stringent tests of tribo-charging models currently available. A second aspect concerns particle shape. In this case steric interactions become important and new types of aggregate behavior can be expected when non-convex particle shapes are considered that can interlock or entangle. However, a general connection between the mechanical response of a granular material and the constituents' shape remains unknown. This has made it infeasible to tackle the "inverse packing problem", namely to start from a given, desired behavior for the aggregate as a whole and then find the particle shape the produces it. We discuss a new approach, using concepts rooted in artificial evolution, that provides a way to solve this inverse problem. This approach facilitates exploring the role of arbitrary particle geometry in jammed systems and invites the discovery and design of granular matter with optimized properties.

Keywords: granular materials, clustering, particle shape, packing, evolutionary computation, 3d printing.
PACS: 41.20.Cv, 45.70.-n, 45.70.Mg, 81.05.Rm

INTRODUCTION

To first order, the behavior of many granular systems is driven by hard surface repulsion, mediated by friction and grain shape.[1,2] However, there are many important industrial and natural settings, ranging from agglomeration in fluidized beds[3] to dust accretion in proto-planetary discs,[4] where more complex interactions become significant. These interactions are usually either short ranged attractions like van der Waals forces or nano-scale liquid bridges, or long-range electrostatic forces that can be either attractive or repulsive. We first discuss how to probe such interactions by removing the effect of gravity. In the second part, we focus on the role of particle shape.

PROBING PARTICLE INTERACTIONS WITH GRANULAR STREAMS

Quantifying attractive interparticle forces has been difficult, with the typical approach being AFM measurements that can only mimic (quasi) static interactions. Recently, however, new ways to tackle this problem have emerged with freely falling granular streams, i.e. gravity driven flows of grains falling from an orifice. By conducting experiments in vacuum and imaging these flows with a co-falling high-speed camera, dynamic grain-grain interactions can be tracked *in-situ* with unprecedented detail.[5,6]

For short-ranged attractions, we recently showed[5,6] that the macroscopic behavior of dense granular streams can be directly linked to the strength of the interparticle force F_{coh}. Figure 1 shows the results of 3d DEM simulations (for details, see [6]). The range of the attractive force was set to 1/1000 of a grain diameter, mimicking van der Waals or capillary forces due to adsorbed molecular layers. For F_{coh}=1 nN, the stream thins and ultimately evolves into a spray of mostly individual particles. For F_{coh}=100 nN, the stream exhibits a breakup similar to the Rayleigh-Plateau instability in liquids. Thus, changing the interaction on the nanoscale leads to dramatically different behaviors on the macroscale.

To make this more quantitative, we systematically increased F_{coh} and tracked how the "droplets" evolve below the nozzle. Fig. 2a shows how the average droplet size, $\langle N \rangle$, develops as a function of distance below the nozzle z for a variety of F_{coh} (N is the number of particles traceable via contacts to a given particle, and the average is over all particles that pass through a given z). For weak cohesion, $\langle N \rangle$ starts

small and grows very slightly before saturating, suggesting subtle agglomeration through collide-and-capture events. As F_{coh} is ramped up, the streams' evolution with z shows a clear peak: capture events are followed by break-up into clusters of 10-100 particles. For the largest F_{coh}, streams leave the hopper as continuous network of >3,000 connected particles, further downstream breaking up into large droplets of several 100 particles each. We find that this trend is independent of the coefficient of restitution e; inelastic collisions mainly help to collimate the stream.

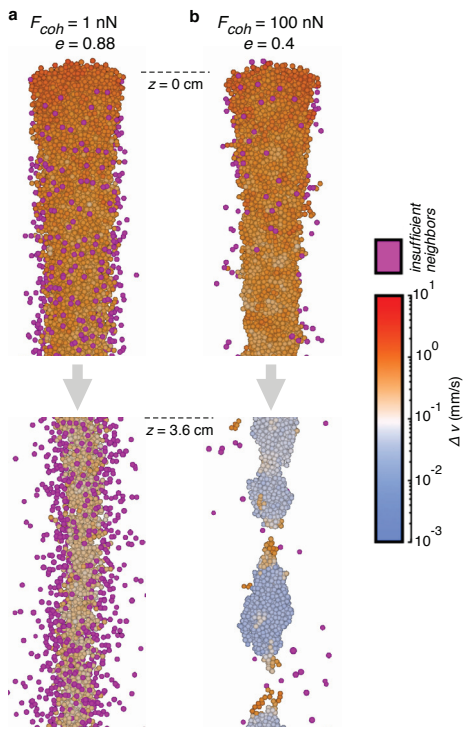

FIGURE 1. Cohesion-driven droplet formation (a) Stream of d=100μm grains falling from D=2mm nozzle with F_{coh}=1nN and inelasticity e=0.88. (b) Same grains/nozzle with F_{coh}=100 nN and e=0.40. Grains are colored by velocity fluctuations relative to nearest neighbors.

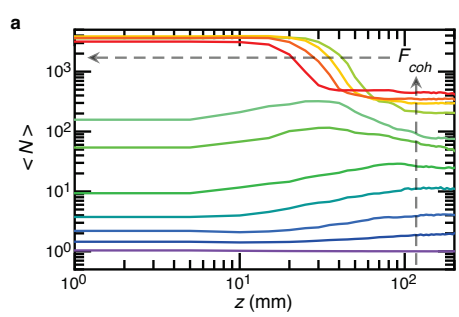

FIGURE 2. Droplet size <N> vs. distance z below nozzle for d=200 μm grains with e=0.61 falling from D=3mm nozzle. Different traces are for increasing F_{coh} as indicated.

Conversely, if the ratio of nozzle to particle diameter is reduced to D/d<15, velocity fluctuations at the orifice become sufficiently effective in preventing collimation and subsequent droplet formation, no matter the value of e. The result is a highly dilute stream, where particles rarely experience collisions.

We have used such dilute streams to probe electrostatic interactions in detail. Fig. 3 shows one of these rare collision events, where a particle, after bouncing several times, gets captured and sticks (note the visible gap after the bounce in the middle image, indicating that the particle separated several microns and thus interacted not via short-range cohesion but longer-range forces). From orbital period and particle size, we estimate a grain charge of ~10^6 electrons.

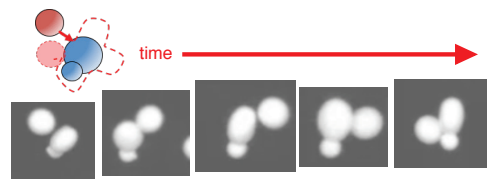

FIGURE 3. Stills from high-speed video showing capture of a single ZrO_2 particle by a 2-particle cluster. The sketch highlights the captured particle's bouncing trajectory.

Such large charge magnitudes in dilute streams cannot arise from collisions during freefall and therefore are present on the grains already before they leave the nozzle (likely from grain-grain collisions and/or rubbing inside the hopper). Applying a uniform horizontal electric field E and tracking non-colliding particle trajectories (Fig. 4, inset), we can obtain the horizontal accelerations a and extract the charge $q=ma/|E|$ of individual grains of mass m.[7] For these experiments we used particle species that charge significantly, such as zirconium dioxide (ZrO_2), since in 100μm glass particles electrostatic forces are two orders of magnitude too small to account for droplet formation.[5]

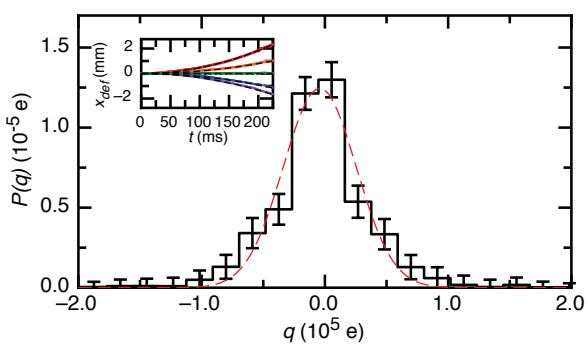

FIGURE 4. Grain charge measurements. Probability density of net grain charge $P(q)$ for d = (300±9)μm ZrO_2 grains falling through an electric field $|E|$ = 79 kV/m. Inset: Sampling of tracked, horizontal particle deflections in the field. Dashed lines are parabolic fits.

In Fig. 4, we plot the charge distribution *P(q)* for tightly size-selected ZrO_2 grains. Its mean value close to zero rules out charge transfer among dissimilar materials as the source of charge. The width of *P(q)* is remarkably large, around 500,000 electron charges, thus *q*-values as estimated for the grains in Fig. 3 are easily available in the tails of *P(q)*. It has been known for some time that tribo-charging between initially neutral grains can lead to net charge build-up even for same-material grains.[8-10] In future experiments, access to the full distribution *P(q)* opens up new opportunities for stringent tests of tribo-charging models that predict a *d*-dependence of the width of *P(q)* and, in particle mixtures, different mean charge for each different size.

DESIGNING GRANULAR AGGREGATE PROPERTIES

Characterizing a granular aggregate's behavior for a *given particle shape* is well established, even if this shape is non-spherical.[11-15] Yet the utility of these advances for actually designing materials is stunted by the fact that the inverse problem is daunting: it still remains a challenge to determine the particle shape that produces a *given desired aggregate behavior*. In fact, since shape is an inexhaustible parameter, systematic exploration of its role in granular aggregates is typically considered infeasible.

A way around this problem starts by rephrasing granular design as an optimization task that can be automated: using only the capacity to check the quality of designs, select from the infinite number of potential configurations those shapes that are appropriately adapted to generate a particular behavior. Efficient solutions to such search and optimization come from evolutionary computing.[16] Here, the key concept is that starting with an initial population of objects, the best performance by a member of the population can be iteratively improved by selecting the fittest objects, mutating them to create offspring, and using the offspring to produce a subsequent generation. Evolutionary computing is emerging as a tool for scientific discovery,[17,18] but so far has not been used for the shape optimization of granular material, likely due to the lack of a particle shape representation that is both unrestrictive and amenable to mutation.

We solve this problem with a representation in which a particle of arbitrary shape is constructed from *n* identical subunits, here taken as spheres.[19] A particle of specific shape is represented by a list of bearings written in sequential order (we call this a 'blueprint'). For each bearing, a ray is drawn that emanates from the origin and is parallel to the bearing. If a sphere is then slid through its center along this ray from infinitely far away towards the origin, then, the location it first comes in contact with the built structure defines the furthest distance along the bearing that still leaves it connected to the previously built shape. A first sphere must be placed at the origin, but by then taking each bearing in sequence, and placing a sphere at these distances, an arbitrary shape can be constructed and used in simulations. Since the resulting shapes resemble chemistry models for molecules, we call them 'granular molecules'.

As a first test of this approach, we employed our evolutionary approach to find, for fixed given *n,* the particle shapes that produce packings with the stiffest response and the softest response to compressive loading. These packings consisted of >2000 granular molecules; their response to mechanical stressing (triaxial test) was simulated with Itasca Pfc3D DEM software and validated by experiments on packings of 3d-printed, mm-sized versions of the particles.[19]

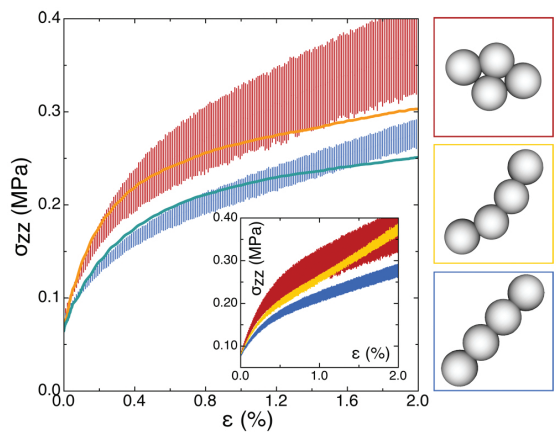

FIGURE 5. Stress-strain curves from triaxial tests on packings of *n*=4 'granular molecules' sketched on the right. Red: Nearly rhombic shape identified as producing the stiffest response (or largest modulus). Blue: Linear configuration producing the softest packings. Solid lines: simulations. Data points: experiments on 3d-printed particles, averaged over 5 trials, with standard deviations for the error bars. Inset: Comparison of experimental data from optimized shapes (from main panel) with suboptimal shape (yellow). Confinement pressure in all cases was 84 kPa.

For *n* up to 5, the range investigated, the softest shapes discovered are always linear molecules while the stiffest shapes are much more compact. Specifically, we find the *n* stiffest shape can be constructed by taking the most compact *n*+1 shape, i.e., the shape whose configuration of *n*+1 spheres minimizes the sum of their distances to the center of mass, and removing one sphere. For example, the most compact shape for *n* = 5 is the triangular bipyramid. Removing one sphere produces the slightly bent, nearly rhombic shape the algorithm discovered as the *n* = 4 stiffest shape. Rules like these provide first steps toward rational shape selection for granular design.

In Fig. 5 we plot stress-strain curves for n = 4 shapes. The significant differences between shapes producing the stiffest and softest response suggest that the evolutionary algorithm makes full use of the configuration space. Over the range the algorithm was optimizing the modulus, i.e., in the limit of small strain, the simulations agree very well with the experiments on 3d-printed specimen. We also tested one suboptimal n = 4 shape: the last slightly bent shape explored by our algorithm before it discovered that completely straight shapes are particularly soft. While the stiffest shape produced packings with modulus 67MPa and the softest with modulus 25MPa, simulation predicted for this suboptimal shape a modulus of 46MPa. The experimental packings were measured to have a modulus of (47 ±1) MPa (Fig. 5 inset), in excellent agreement.

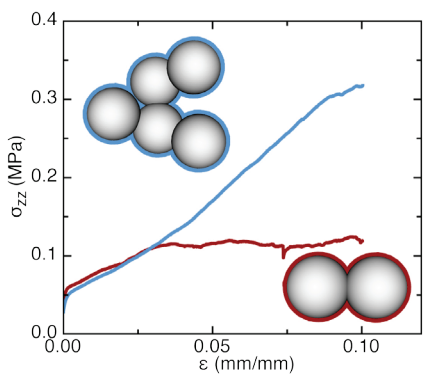

FIGURE 6. Experimental stress-strain curve for n = 5 particle designed to produce strain-stiffening aggregate behavior (blue). Note the presence of a new inflection point, which leads to positive curvature, in contrast to all other shapes that strain-soften, exemplified here by experimental data on dimer particles under the same conditions (red). Confinement pressure for these tests was 35 kPa.

As a next test, we used the evolutionary strategy to find a shape that would produce strain-stiffening, i.e. maximize the second derivative of stress with respect to strain. This is a hard task for granular packings since their aggregate response is generically strain-*softening*: they get weaker the more they are compressed and finally fail dramatically, typically by shear banding. In prior work, only granular polymers consisting of flexible linear chains had been observed to strain stiffen, if long enough to entangle.[20]

The evolutionary strategy led to the discovery of a unique, rigid particle that, with just 5 constituent spheres arranged like a 'wishbone', produces a concave-upward dependence for σ(ε) (Fig. 6). What is more, in aggregate this small granular molecule achieves remarkable self-confinement under load: it can sustain stress levels 10 times larger than the confining pressure, yet does not fail up to almost 10% strain, an order of magnitude larger than for single spheres under the same conditions.

The approach discussed here is a new way to design granular aggregate behavior via the shape of individual particles. It can be used for optimizing a wide range of static as well as dynamic aggregate characteristics, from packing fraction to flowability, or propensity to jam. In addition, beyond optimizing single parameters such as modulus, strength or toughness, one can envision optimization with respect to whole stress-strain curves, including failure modes.

ACKNOWLEDGMENTS

This work was supported by the NSF MRSEC program under DMR-0820054. Additional support came from the US Army Research Office through W911NF-12-1-0182.

REFERENCES

1. H. M. Jaeger, S. R. Nagel, R. P. Behringer, *Rev. Mod. Phys.* **68**, 1259 (1996).
2. J. Duran *Sands, Powders, and Grains: An Introduction to the Physics of Granular Materials*, Berlin: Springer, 1999.
3. J. W. Chew *et al.*, *Chem. Eng. Sci.* **68**, 72 (2012).
4. T. Poppe, R. Schrapler, *Astron. Astrophys.* **438**, 1 (2005).
5. J. R. Royer *et al.*, *Nature* **459**, 1110 (2009).
6. S. R. Waitukaitis, H. F. Grutjen, J. R. Royer, H. M. Jaeger, *Phys Rev E* **83**, 051302 (2011).
7. S. R. Waitukaitis, H. M. Jaeger, *Rev. Sci. Instr.* **84**, 025104 (2013).
8. P. E. Shaw, *Nature* **118**, 659 (1926).
9. D. J. Lacks, N. Duff, S. K. Kumar, *Phys. Rev. Lett.* **100**, 188305 (2008).
10. J. F. Kok, D. J. Lacks, *Phys. Rev. E* **79**, 051304 (2009).
11. S. A. Galindo-Torres, F. Alonso-Marroquin, Y. C. Wang, D. Pedroso, J. D. Munoz Castano, *Phys. Rev. E* **79**, 060301 (2009).
12. A. Haji-Akbari *et al.*, *Nature* **462**, 773 (2009).
13. T. Pöschel, T. Schwager, *Computational granular dynamics: models and algorithms*, Berlin: Springer, 2005.
14. I. Zuriguel, T. Mullin, *Proc. Royal Soc. A* **464**, 99 (2008).
15. A. Jaoshvili, A. Esakia, M. Porrati, P. M. Chaikin, *Phys. Rev. Lett.* **104**, 185501 (2010).
16. A. E. Eiben, J. E. Smith, *Introduction to evolutionary computing*, New York: Springer, 2003.
17. A. O. Lyakhov, A. R. Oganov, *Phys. Rev. B* **84**, 092103 (2011).
18. E. Bianchi, G. Doppelbauer, L. Filion, M. Dijkstra, G. Kahl, *J. Chem. Phys.* **136**, 214102 (2012).
19. M. Z. Miskin, H. M. Jaeger, *Nature Materials* **12**, 326–331 (2013).
20. E. Brown, A. Nasto, A. G. Athanassiadis, H. M. Jaeger, *Phys. Rev. Lett.* **108**, 108302 (2012).